Design and simulation of Zeonex Based Suspended Microstructure Photonic Crystal Fiber for Chemical Sensing Application

Md. Rakibul Islam[1], Tabassum Jannat Ritu[1], Saeed Mahmud Ullah[2] *

[1]*Department of Electrical and Electronic Engineering, Mymensingh Engineering College, Mymensingh, Bangladesh*

[2]*Department of Electrical and Electronic Engineering, University of Dhaka, Dhaka, Bangladesh*

**E-mail: ullahsm@du.ac.bd*

Received on 12 August 2022, Accepted for publication on 21 February 2023

ABSTRACT

Over the last few years for sensing applications in terahertz regime photonic crystal fiber (PCF) has gained attention quite extensively. The optical characteristics of photonic crystal fiber can be controlled by fine-tuning of the structural parameters like core radius and effecctive area. In this context, a terahertz sensor based on a hollow-core photonic crystal fiber has been developed for chemical identification in the terahertz frequency range with very low loss. The proposed structure contains hexagonal manner sectored suspension type cladding and hexagonal manner sectored core region, all the sector are formed by zeonex based struts. To investigate the optical characteristics of developed design, finite element method (FEM) based COMSOL multiphysics v.5.4a software has been used. The simulation result shows the sensitivity of 83.37% and 83.63% at the optimum condition in x-polarization mode for ethanol and benzene respectively with low effective material loss of 0.0291 cm^{-1} and low confinement loss of 1.87×10-13 $cm^{-1.}$ Moreover, the developed design implementation is possible in the existing fabrication method. Physical features and comparative performance analysis are also showed in this research.

Keywords: Effective material loss, confinement loss, fiber sensor, sensitivity, suspended.

1. Introduction

Benzene and ethanol are widely used in industrial chemicals. Benzene is found in crude oil and is a major part of gasoline. In industry, it is used to make plastics, resins, synthetic fibers, rubber lubricants, dyes, detergents, drugs etc. Ethanol is used extensively as a solvent in the manufacture of varnishes and perfumes as a preservative for biological specimens and as a fuel and gasoline additive. Benzene and ethanol cause harmful effects on the bone marrow and can cause a decrease in red blood cells, leading to anemia and many long term damage to the human body. It can also cause excessive bleeding and can affect the immune system, increasing the chance of infection. An accurate amount of chemical reaction in the industry provides human safety as well as production efficiency. So the amount of benzene and ethanol concentration in every step of use needs to be precise. So the accurate detection of those chemicals is a very important factor. During the last several decades, development of optical fiber technology blessed the telecommunication sector [1, 2] and chemical analyst sensing area [3, 4]. Photonic crystal fiber (PCF) is the smart version of optical fiber and has some identical properties [5]. In the year of 1996, Knight first introduced PCF for its novel characteristics [6]. PCF is a special kind of fiber where artificial frequent capillaries occur. Characteristics of optics are mainly guided by the size and quantity of microstructure capillaries of air holes [7] and several structural diversities. In recent years sensing chemical and gas analysis through photonic crystal fiber has become a hot topic among the researchers. To increase the performance of photonic crystal fiber in the field of chemical sensing, researchers have given much effort on this topic [8, 9]. Sensing characteristics of the fiber base sensor is varying with the position and size of air holes in the core region as well as the cladding region [10, 11]. Confinement loss, sensitivity dispersion, and effective material loss (EML) are considered as main optical properties among all their optical properties for liquid and chemical identification. Birefringence of high value is always recommended for various applications [12,13]. Researchers around the world are conducting research to maximize the sensitivity of PCF and minimize the confinement loss [14]. As a result, different types of microstructure core and cladding based PCF have been introduced with high sensitivity along with low confinement loss. A few years ago PCF sensor with elliptical type air hole at the center position was proposed by Asaduzzaman et al where relative sensitivity of 49.71% for ethanol along with birefringence of 0.0015 and confinement loss of 2.75 × 10^{-10} dB/m were published [15]. In 2017 a folded shaped porous core silicon-based PCF was proposed whose relative sensitivity was 69% with 5×10^{-11} dB/cm confinement loss for benzene [16]. In 2019, a hexagonal shaped and hybrid microstructure PCF was proposed by Md. Ahasan Habib in which relative sensitivity was reported to be 78.07% with low confinement loss of 7.4×10-11 cm^{-1} for benzene and ethanol [17]. In this work, a terahertz sensor based on a hollow-core photonic crystal fiber has been proposed for chemical identification in the terahertz frequency range with very low loss. The proposed structure contains hexagonal manner sectored suspension type cladding and hexagonal manner sectored core region,

2. Physical Insight of The Proposed Sensor

Fig.1 represents the 2D transverse cross-sectional view of the proposed PCF structure as well as an amplified view of the core area. The cladding of the reported PCF is composed of six symmetrical air slices which are organized circularly.

The core portion is also formed by six equal size and same pattern square holes. The main purpose of choosing this type of structure is to decrease the interaction of light with the background material which helps to reduce losses and improve sensitivity. In the proposed PCF structure, the selected length and height of air slice are L=605 µm and h=766 µm respectively at an optimum core radius of C=170 µm. Cladding and core Strut width of the PCF is considered 14µm and 12µm as highest to manage fabrication tolerance. Six triangular-shaped core air hole is settled between the inner side of the core circle and outer side of the core air hole. For ignoring unwanted electromagnetic radiation by the environment, a perfectly matched layer (PML) has been taken as a boundary condition to the outer structure of the fiber. As background material in fiber, zeonex is preferred as it shows relatively better characteristics at 0.1 THz to 3THz with constant refractive index of 1.53.

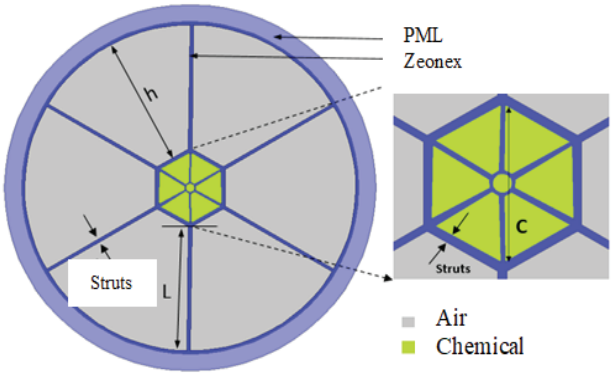

Fig.1. Cross section of the proposed terahertz PC-PCF sensor with its amplified version of the core.

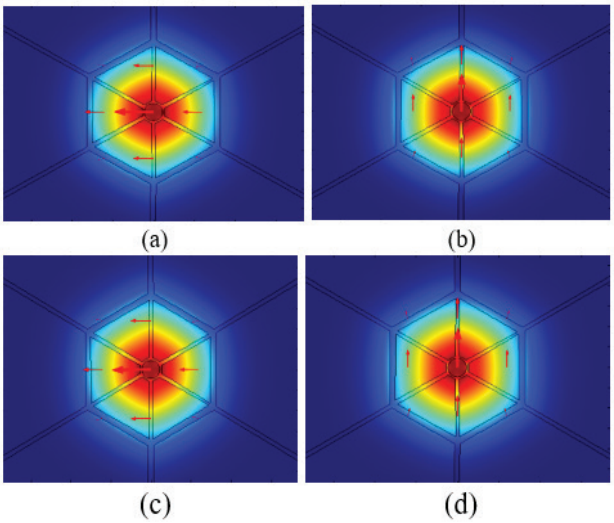

Fig. 2. E-field distribution for (a) x-polarization, benzene (b) y-polarization, benzene (c) x-polarization, ethanol (d) y-polarization, ethanol.

3. Simulation Results and Discussion

Simulation has been carried out using COMSOL Multiphysics for benzene and ethanol. The electrical field circulation of the PCF for both chemicals is shown in Fig. 2. The tight confinement of light through the center region of the proposed structure is confirmed by Fig. 2 for both chemicals.

Modified Beer-Lambert law has been used to resolve the sensing capacities of the proposed structure, which is determined by the interaction between the light and aimed chemical samples. The following mathematical equation represents the characteristic of this situation [18]

$$I(f) = I_0(f)exp[-r\alpha_m I_C] \quad (1)$$

Here, I(f) indicates the intensities of light at the presence of chemical and I_0(f) indicates at the absence of chemical. Co-efficient of sensitivity and material absorption are denoted by r and α_m respectively. Operating frequency and light in the fiber are denoted by f and Ic.

The absorbance can be calculated by [19]

$$A = \log\left(\frac{I(f)}{I_0(f)}\right) = -r\,\alpha_m I_C \quad (2)$$

The relative sensitivity r to be expressed by the following Eq. [20],

$$r = \frac{n_r}{Re[n_{eff}]} \times k \quad (3)$$

Where, n_r stands for the refractive index of the chemical analyte to be detected. Using this equation, the refractive index of benzene and ethanol are found to be 1.366 and 1.354 respectively. Here, n_{eff} represent the guided mode effective refractive index and K is the total power fraction inside the core section [21], where,

$$K = \frac{\int_{sample} R_e(E_m H_n - E_n H_m)\,dx\,dy}{\int_{total} R_e(E_m H_n - E_n H_m)\,dx\,dy} \quad (4)$$

In above equation H_m and E_m represent the transverse component of magnetic field and electric field respectively. Also H_n and E_n are denoted for longitudinal component of magnetic field and electric field respectively.

Fig. 3 & Fig. 4 showed relative sensitivity of the suspended design for both ethanol and benzene at optimum ±2 condition for x-polarization mode. Optimum±2 condition means all the numerical parameter of the proposed structure varied this percentage excluding PML. ±2% variation has been taken because variation of the parameter value can happen during standard fabrication process. Fig. 3 & Fig. 4 show the maximum sensitivity to be 83.37% and 83.63 % for ethanol and benzene respectively at f=1.5THz. As it can be seen from the figures that sensitivity becomes stable around 1.5 THz, so it has been considered as the optimum frequency. This result is better than most recently reported research work [22-24].

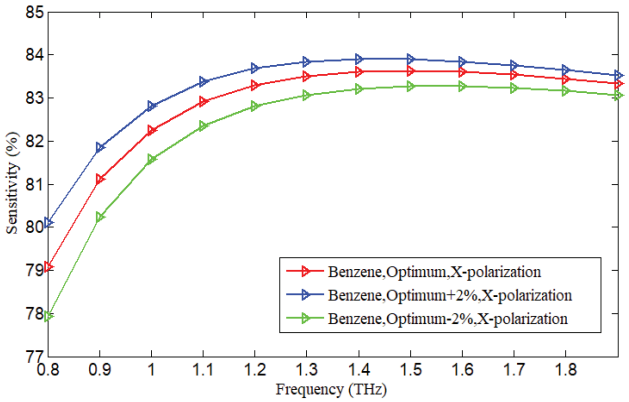

Fig. 3. Relative sensitivity of benzene with respect to frequency for x-polarization of reported PCF

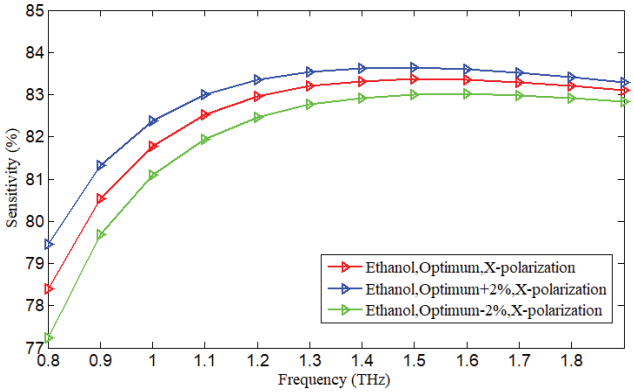

Fig. 4. Relative sensitivity of ethanol with respect to frequency for x-polarization of reported PCF

Fig. 5 & Fig. 6 represent the relative sensitivity of proposed structure for both ethanol and benzene at optimum frequency for y-polarization mode with optimum ±2% condition. Figure confirmed that 1.5THz frequency is the maximum sensitivity area for both the chemicals. Sensitivity increases and decreases slightly in numerical ±0.8% of maximum sensitivity.

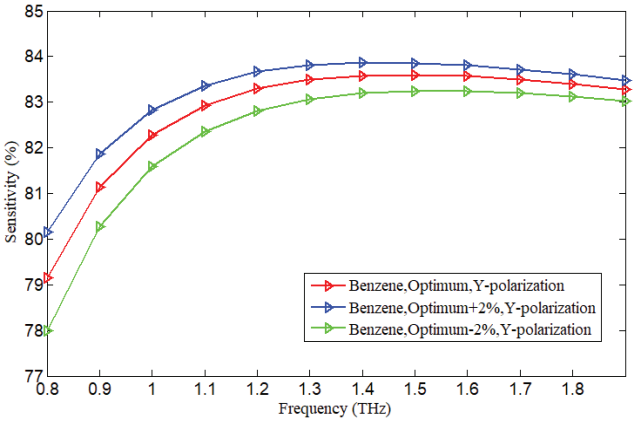

Fig. 5. Relative sensitivity of benzene with respect to frequency for y-polarization of reported PCF

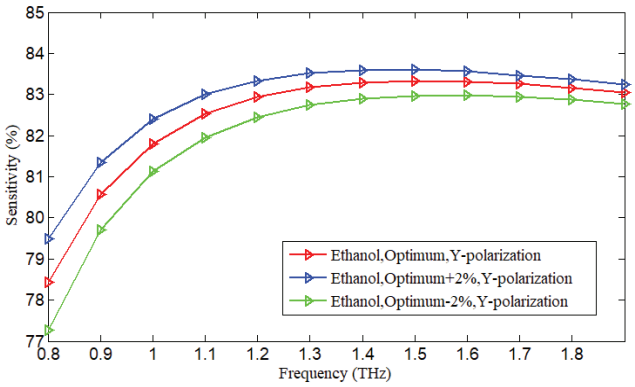

Fig. 6. Relative sensitivity of ethanol with respect to frequency for y-polarization of reported PCF

Confinement loss of HC-PCF can be calculated from the following equation [27].

$$\alpha_{CL} = 8.686 \times \frac{2\pi f}{c} \mathrm{Im}(n_{eff}) \quad (5)$$

Here, c is the velocity of light at free space, f is operating frequency and $Im(n_{eff})$ is the imaginary part of the effective refractive index of the guided mode.

Fig. 7 shows the confinement loss with respect to frequency. As can be seen, confinement loss decreases with the increase of frequency since the mode field starts to confine tightly in the core area with increasing frequency. At the optimum reported condition confinement loss found to be 1.87×10-13 cm^{-1} and 2.46×10-13 cm^{-1} for benzene and ethanol respectively which are better than previously published research work [25-27].

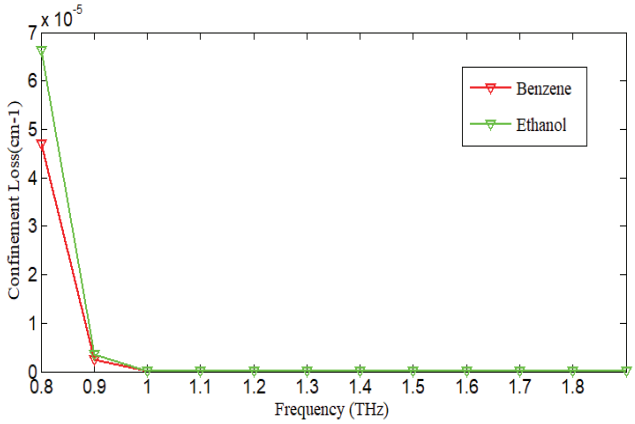

Fig. 7. Confinement loss of proposed PCF with variation of frequency for ethanol and benzene.

At the time of operation, another kind of optical fiber loss is the effective material loss (EML). This loss happened due to the background polymer material. It is one of the main concerns to minimize material loss by choosing a good background material. EML of the proposed structure can be calculated by the following equation [28].

$$\alpha_{eff} = \sqrt{\frac{\varepsilon_0}{\mu_0}}\left(\frac{\int_{mat} n_{mat}\,|E|^2\alpha_{mat}\,dA}{\int_{all} S_z dA}\right) \quad (6)$$

Where α_{eff} is denoted for EML, ϵ_0 and μ_0 indicate the relative permittivity and relative permeability respectively in free space, n_{mat} is denoted for refractive index of background material, α_{mat} stands for absorption loss of zeonex , S_z is the sign pointing vector of z-component.

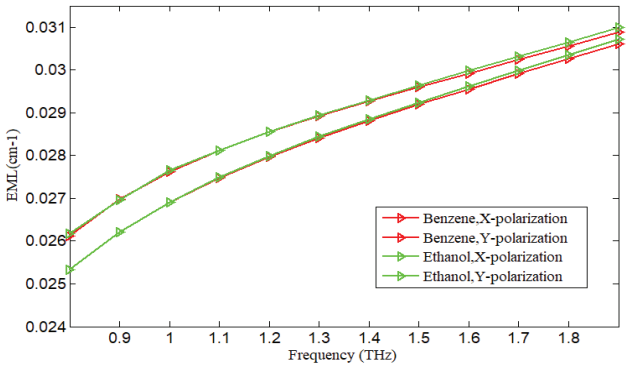

Fig. 8. Effective area of suggested PCF according to frequency variation for ethanol and benzene.

Figure 8 represents the EML of proposed fiber with respect to frequency. It gives the confirmation of effective material loss to be increased with increase of frequency and EML of benzene is slightly lower than ethanol. At the frequency 1.5 THz EML calculated for both benzene and ethanol is 0.0290 cm^{-1} and 0.0291 cm^{-1} respectively. This value is lower than previously reported work [26].

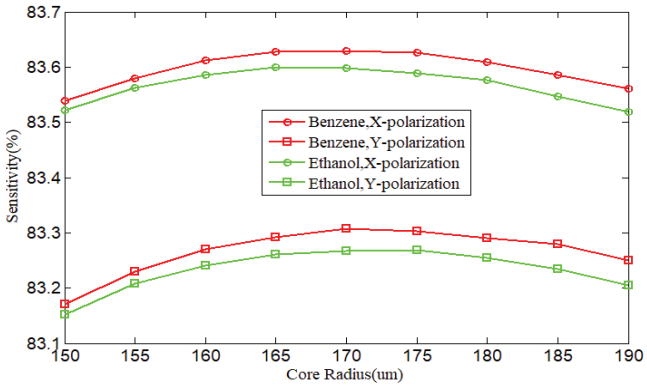

Fig. 9. Sensitivity of benzene and ethanol for both polarization mode with respect to core radius.

Now the relative sensitivity of the proposed fiber for ethanol and benzene are showed in figure 9 for both x and y polarization mode with respect to core radius at frequency 1.5THz. It shows that for both chemicals and for both polarization, core radius of 170 µm gives the maximum sensitivity. Figure 10 represents the confinement loss with respect to the core radius. It states that confinement loss decreases with increment of core radius until 170 µm, from where it becomes almost constant. The value of the confinement loss at 170 µm is found to be 1.87×10^{-13} cm^{-1} and 2.46×10^{-13} cm^{-1} for benzene and ethanol respectively.

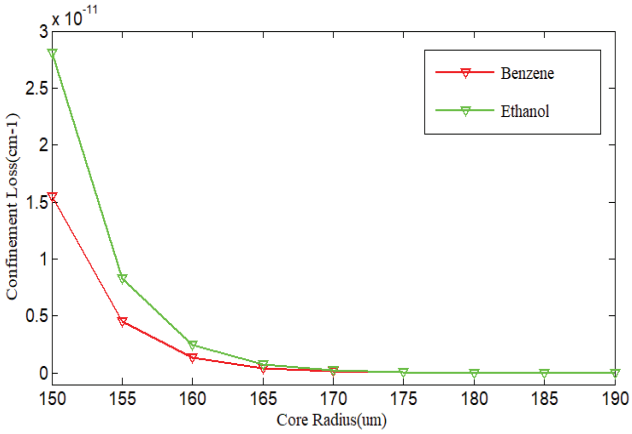

Fig. 10. Confinement loss for benzene and ethanol with variation of core radius.

For the implementation of PCF, THz guided lightwave faces another loss named bending loss which can be determined by following equation [29],

$$\alpha_{BL} = \frac{1}{8}\sqrt{\frac{2\pi}{3}\times\frac{1}{\beta A_{eff}}}F\left[\frac{2}{3}R_b\frac{\left(\beta^2-\beta_{Cl}^2\right)^{2/3}}{\beta^2}\right] \quad (7)$$

where, effective area is represented by A_{eff}, R_b is denoted for bending radius, propagation constant is $\beta = 2\pi n_{co}/\lambda$, and $\beta_{cl} = 2\pi n_{cl}/\lambda$, core refractive index is n_{co} and cladding refractive index is n_{cl}

The bending loss with respect to frequency is shown in Fig. 11 at R_b=1 cm and R_b=2 cm for both ethanol and benzene. It confirms that bending loss decreases with increasing frequency. Numerical value for the reported PCF is negligible which is 7.31804×10^{-36} cm^{-1} and 1.35782×10^{-34} cm^{-1} for benzene and ethanol at R_b =1 cm at 1.5 THz . For the R_b=2 cm, bending loss is 6.56878×10^{-72} cm^{-1} and 2.41875×10^{-69} cm^{-1} at 1.5 THz.

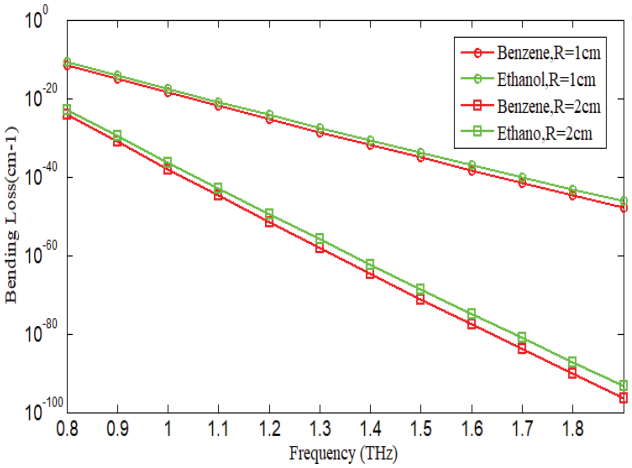

Fig. 11. Bending loss of proposed PCF for benzene and ethanol at R_b=1cm and R_b=2cm

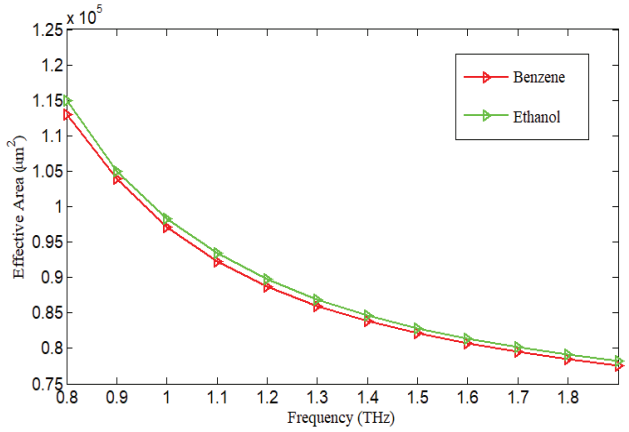

Fig. 12. Effective area `of suggested PCF according to frequency variation for ethanol and benzene.

Effective area is the core area covered by interaction of light. High value of effective area is always appreciated for PCF which depends on the strut size and air hole. Reported fiber effective area is calculated by following expression [30],

$$A_{eff} = \frac{[\int I(r)rdr]^2}{[I^2(r)dr]^2} \quad (8)$$

Where $I(r) = [Et]^2$ stands for the transverse electric intensity distribution of total cross-section of the fiber. The effective area of the reported photonic crystal fiber is presented in Fig. 12 which shows that a decrease of effective area increases the operating frequency. Another property of photonic crystal fiber is dispersion. Low and flattened dispersion is always recommended for good optical fiber as the transmission depends on dispersion. Effective refractive index directly affects the dispersion. This is also a reason behind taking zeonex as host material as it has a constant refractive index up to 3 THz. Waveguide dispersion of the proposed fiber can be determined by following equation [31],

$$\beta_2 = \frac{2}{c}\frac{d\, n_{eff}}{dw} + \frac{w}{c}\frac{d^2 n_{eff}}{dw^2} \quad (9)$$

Where w = angular frequency, speed of light is c at free space. Effective refractive index of proposed optical fiber is denoted by n_{eff}. The dispersion of the reported optical fiber is shown in Fig. 13 with the variation of frequency. It is seen that suggested PCF has enough flattened behavior from 1.4 THz to 1.9THz frequency. Numerically, dispersion of the suggested optical fiber is 0.55±0.10 ps/THz/cm for both ethanol and benzene. Comparison among existing photonic crystal fibers and the proposed PCF is shown in Table 1. From Table 1 it is clear that the proposed PCF achieved some noticeable improvement in sensitivity of chemicals as well as optical fiber loss.

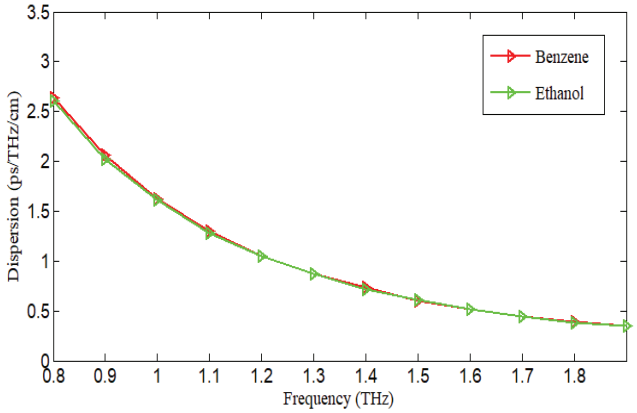

Fig. 13. Dispersion of suggested fiber for both chemical with respect to different frequency.

Table 1: Comparison among previously Reported and proposed designs.

Year	Sensitivity (%)	CL (dB/m)	EML (cm^1)	Frequency (THz)	Ref.
2017	53.35%	1.6×10^{-10}	---	1.33	[22]
2018	57.91%	1.6×10^{-3}	---	1.33	[21]
2017	65.18%	5×10^{-9}	---	1.55	[23]
2019	78.5 %	1.15×10^{-9}	0.028	1.7	[24]
2019	79.2%	3.2×10^{-9}	0.0389	1.5	[26]
Proposed	83.6%	8.11×10^{-12}	0.029	1.5	

4. Fabrication options

There are different kinds of fabrication methods invented for symmetrical and asymmetrical structure. Stack and draw sol-gel, capillary extrusion, and 3D printing process are made their place at the microprocessing sector [32,33]. National Oceanography Centre and optoelectronics research center Southampton, UK exposed the extrusion and 3D printing fabrication process for suspended geometry [34]. As our geometry formed with 6 symmetrical sectored core and cladding in a circular manner, 3D printing and extrusion fabrication process should be suitable for the proposed suspended geometry.

5. Conclusion

A different kind of suspended geometry is established with numerical analysis for developed PCF. For suggested optical fiber design, numerical result gives the provenance of high preference. Proposed geometry shows extremely low confinement loss of 1.8×10^{-12} cm^{-1} and very low effective material loss of 0.029 cm^{-1}. It also showed a high sensitivity of 83.6% and 83.3% for benzene and ethanol respectively. Moreover proposed microstructure geometry can be easily fabricated by existing technology. So we can hope, it will bring significant development in the sector of PCF base chemical detection and THz wave propagation.

References

1. L D Coelho, O Gaete, N Hanik. An algorithm for global optimization of optical communication systems. *AEÜ-International Journal of Electronics and Communications*, 63(7): 541–550, 2009.
2. B. Furch, Z. Sodnik, H. Lutz, Optical communications in space-a challenge for Europe. *AEÜ-International Journal of Electronics and Communications*, 56(4): 223–231, 2002.
3. R. C. Jorgenson, S. S. Yee, A fiber-optic chemical sensor based on surface plasmon resonance. *Sensors and Actuators B, Chemical*, 12(3): 213–220, 1993.
4. Z. Xu, X. Chen, H. N. Kim, J. Yoon, Sensors for the optical detection of cyanide ion. *Chemical Society Reviews*, 39(1): 127–137, 2010.
5. X. Sang, P. L. Chu, and C. Yu, "Applications of nonlinear effects in highly nonlinear photonic crystal fiber to optical communications," *Optical and Quantum Electronics*, 37(10): 965–994, 2005.
6. T. A. Birks, J. C. Knight, and P. S. J. Russell, "Endlessly single-mode photonic crystal fiber," *Optics Letters*, 22(13): 961–963, 1997.
7. M. Morshed, M. H. Imran, T. K. Roy, M. S. Uddin, and S. M. A. Razzak, "Microstructure core photonic crystal fiber for gas sensing applications," *Applied Optics*, 54(29): 8637–8643, 2015.
8. J. M. Fini, Microstructure fibres for optical sensing in gases and liquids. *Measurement Science & Technology*, 15(6): 1120– 1128, 2004.
9. X. D. Wang, O. S. Wolfbeis, Fiber-optic chemical sensors and biosensors (2013–2015). *Analytical Chemistry*, 88(1): 203–227, 2016.
10. X. Yang, Y. Lu, B. Liu, J. Yao, Analysis of graphene-based photonic crystal fiber sensor using birefringence and surface plasmon resonance. *Plasmonics*, 12(2): 489–496, 2017.
11. R. Otupiri, E. K. Akowuah, S. Haxha, H. Ademgil, AbdelMalek F, Aggoun A. A novel birefrigent photonic crystal fiber surface plasmon resonance biosensor. *IEEE Photonics Journal*, 6(4): 1–11, 2014.
12. K. Saitoh, M. Koshiba, Single-polarization single-mode photonic crystal fibers. *IEEE Photonics Technology Letters*, 15(10): 1384–1386, 2003.
13. M. Yamanari, Fiber-based polarization-sensitive Fourier domain optical coherence tomography. *Dissertation for the Doctoral Degree. Tsukuba: University of Tsukuba.*
14. N A. Mortensen, Effective area of photonic crystal fibers. *Optics Express*, 10(7): 341–348, 2002.
15. S. Asaduzzaman, K. Ahmed, T. Bhuiyan, and T. Farah, "Hybrid photonic crystal fiber in chemical sensing," *SpringerPlus*, vol. 5, no. 748, pp. 1-11, 2016.
16. B. K. Paul, K. Ahmed, S. Asaduzzaman, and M. S. Islam, "Folded cladding porous shaped photonic crystal fiber with high sensitivity in optical sensing applications: Design and analysis," *Sens. and Biosens. App*., vol. 12, pp. 36-42, 2017.
17. Md. Ahasan Habib, Md. Selim Reza," Hybrid-core microstructure fiber for chemical identification in terahertz regime" *ICASERT 2019*.
18. M.S. Islam, J. Sultana, A.A. Rifat, A. Dinovitser, B.W.-H. Ng, D. Abbott, Terahertz sensing in a hollow core photonic crystal fiber, *IEEE Sensor Journal* 1558–1748 c, 2018.
19. H. Ademgil, Highly sensitive octagonal photonic crystal fiber based sensor, *Optik* 125 (20) 6274–6278, 2014.
20. M.S. Islam, J. Sultana, K. Ahmed, A. Dinovitser, M.R. Islam, B.W.-H. Ng, D. Abbott, A novel approach for spectroscopic chemical identification using photonic crystal fiber in the terahertz regime, *IEEE Sens. J.* 18 (2) 575–582, 2018.
21. Ashish Kumar Ghunawat, Sharad Sharma, Sourabh Sahu, Ghanshyam Singh, Highly Sensitive Octagonal Photonic Crystal Fiber for Ethanol Detection, *Springer Optical and Wireless Technologies* (pp 457-466, volume 546).
22. M. F. H. Arif, and M. J. H. Biddut, "A new structure of photonic crystal fiber with high sensitivity, high nonlinearity, high birefringence and low confinement loss for liquid analyte sensing applications," *Sens. and Biosens. App.,* vol. 12, pp. 8-14, 2017.
23. B. K. Paul, K. Ahmed, S. Asaduzzaman, and M. S. Islam, "Folded cladding porous shaped photonic crystal fiber with high sensitivity in optical sensing applications: Design and analysis," *Sens. and Biosens. App.,* vol. 12, pp. 36-42, 2017.
24. Md. Ahasan Habiba , Md. Shamim Anowera , Lway Faisal Abdulrazakb , Md. Selim Rezac,Hollow core photonic crystal fiber for chemical identification in terahertz regime, *ELSIVER, Optical Fiber Technology,* Volume 52, 101933, November 2019.
25. G. Woyessa, A. Fasano, C. Markos, et al., Zeonex microstructured polymer optical fiber: fabrication friendly fibers for high temperature and humidity insensitive Bragg grating sensing, *Opt. Mater. Express 7* (1) 286–295, 2017.
26. Md. Ahasan Habib, Md. Selim Reza, Hybrid-core microstructure fiber for chemical identification in terahertz regime, *ICASERT 2019.*
27. M.S. Islam, J. Sultana, K. Ahmed, M.R. Islam, A. Dinovister, B.W.H. Ng, D. Abbott, A novel approach for spectroscopic chemical identification using photonic crystal fiber in the terahertz regime, *IEEE Sens. J.* 18 (2) 575–582, 2018.
28. M.S. Islam, J. Sultana, A. Dinovitser, M. Faisal, M.R. Islam, B.W.-H. Ng, D. Abbott, Zeonex-based asymmetrical terahertz photonic crystal fiber for multichannel.
29. I.K. Yakasai, P.E. Abas, H. Suhaimi, F. Begum, Low loss and highly birefringent photonic crystal fibre for terahertz applications, *Optik - International Journal for Light and Electron Optics 206*, 2020.
30. M.M. Rahman, F.A. Mou, M.I.H. Bhuiyan, M.R. Islam, Design and characterization of a circular sectored core cladding structured photonic crystal fiber with ultra-low EML and flattened dispersion in the THz regime, *Opt. Fiber Technol. 55*, 102158, 2020.
31. K. Ahmed, F. Ahmed, S. Roy, B.K. Paul, M.N. Aktar, D. Vigneswaran, M.S. Islam, Refractive Index Based Blood Components Sensing in Terahertz Spectrum, *IEEE Sensors Journal 19* (9) 2019.
32. H. Ebendorff-Heidepriem, J. Schuppich, A. Dowler, L. Lima-Marques, T.M. Monro, 3D-printed extrusion dies: a versatile approach to optical material processing, *Opt. Mater. Exp 4 (8)*, 1494–1504, 2014.
33. Z. Liu, C. Wu, M. Vincent Tse, H. Yaw Tam, Fabrication, characterization, and sensing applications of a high-birefringence suspended-core fiber, *Journal of Lightwave Technology 32 (11)*, 2014.
34. W. Talataisong, R. Ismaeel, S.R. Sandoghchi, T. Rutirawut, G. Ntopley, M. Beresna, G. Bambilla, Novel method for manufacturing optical fiber: extrusion and drawing of microstructured polymer optical fibers from a 3D printer, *Optics Express 26 (24)*, 2018.